Highly Transparent Liquid Marble in Liquid (HT-LMIL) as 3D Miniaturized Reactor for Real-time Bio-/Chemical Assays

Zhijian Zhao,[1+] Xiaoxue Yao,[2,+] Bo Shi,[1] Sreepathy Sridhar[3], Yuan Pu,[1] Stevin Pramana[4], Dan Wang,[1,*] Steven Wang[2,*]

[1] State Key Laboratory of Organic Inorganic Composites, Beijing University of Chemical Technology, Beijing 100029, China

[2] Department of Mechanical Engineering, City University of Hong Kong, Hong Kong, China

[3] Department of Mechanical and Constructions Engineering, Northumbria University, United Kingdom

[4] School of Engineering, Newcastle University, Newcastle upon Tyne, United Kingdom

[+] These authors contributed equally to this work.

[*] Corresponding authors: D. Wang (wangdan@mail.buct.edu.cn), S. Wang (steven.wang@cityu.edu.hk)

Abstract

Traditional liquid marbles (LMs), are liquid droplets encapsulated by hydrophobic particles offering special three-dimensional (3D) stereo-architectures with structurally and functionally confined environment. However, the particle armors impede optical characterization in chemical analysis and process monitoring for fluid reactions. For the first time, we manipulate the liquid-solid interface by the paradigm of liquid marbles in liquid (LMIL) strategy, in which LMs are coated by diverse particles immersed in liquid mediums rendering optically transparent micro-reactor system without compromising on its intuitive functional potential. We demonstrated comparable transmittance of HT-LMIL towards naked water droplet *via* UV-vis absorption spectroscopic detection. Besides, its function as an oil immersion lens gives higher resolution in optical spectroscopic characterization. The high optical transparency of LMIL enables real-time and *in situ* monitoring of yeast cell's proliferation and viability *via* layer-by-layer, encouraging them to differentiate in suspension without anchoring. Such multifaceted characteristics of HT-LMIL based platform offer optically transparent and functionally promising micro/bio-reactors with future explorations for high-throughput chemical assays.

Keywords

Liquid marble; 3D miniaturized reactor; LMIL; Cell culture; Chemical assays

Introduction

Liquid marbles (LMs), are distinguished by a stable liquid nucleus protected by hydrophobic nanoparticles to isolate internal fluid from mixing with the external fluidic environment.[1] As non-wetting liquid droplets, they promise superior performance on mobility,[2] elasticity,[3] and stability.[4] The liquid marble reactor also withholds many advantages such as minimized use of chemical reagents, precisely controlled and intensified reaction conditions, and momentary reaction time.[5-8] Thereafter, LM-based technologies have been exploited for extensive application in microreactors,[9,10] microfluidic control,[11] bioreactors,[12] and other practical applications.[13-15] Moreover, the fundamental characteristics of internal fluid entrapped and tailored coating particles enable the LMs responding to various stimuli such as pH,[16] thermal, light,[17,18] magnetism,[19] electric field[20] and others.[21] Such a LM based platform has been widely developed for applications in gas sensing,[22] water pollution detection, and blood typing.[23]

Traditional LMs adopt various nanoparticles to construct multifunctional hydrophobic shells enabling LMs with prominent potential as lab-in-a-drop.[24] Such miniaturized strategy has apparent advantages for high-throughput chemical analysis,[25] which has gained pronounced interest in the trace analysis field.[26] Study by Xue et al. that employed magnetic particle-coated LMs was directed towards quantitative analysis and purification with on-demand opening and closing bifunctionality under magnetic field to replace the internal liquid without risk of contamination.[27] LMs also serve as the three-dimensional (3D) micro-bioreactors for *in vitro* drug screening and

regenerative medicine study.[28] Aalders et al. demonstrated a fumed silica powder stabilized LM as an artificial cell culture environment to create 3D cardiospheres within 24 h.[29] However, since armored by the lightproof shell, these LMs can only execute downstream analyses *via* destructive extraction of objects, restricting their on-line measurement and continuous recyclability.[30]Traditionally, the optical transparency of LMs can be improved by manipulating the type, size, and processing of hydrophobic particles shell, which not only endows structural protection but also benefits the monitoring of inner dynamic changes.[31-35] Bhosale et al. reported that microparticles were light-proof, while particles at the nanoscale can form LMs with high transparency.[36] Therefore, Nguyen et al. presented a LM-based digital-imaging colorimetry strategy to study the enzymatic starch hydrolysis in real-time without destruction, due to the excellent optical transparency of silica nanoparticles.[37] Lin et al. also exhibited monolayer silica nanoparticles coated transparent LMs towards real-time monitoring of embryonic cells.[38] However, these coatings are quite barren in functions and require complex preparation processes. In addition, the porosity of coating incurs rapid evaporation of constituents in the air, reducing the accuracy of LM based-colorimetry and degrading the durability of LMs for translational research.[39]

Herein, we leverage on a facile, universal, and low-cost liquid marble in liquid (LMIL) strategy to break through the inherent opaqueness and evaporation drawbacks of LMs, realizing the real-time LM internal fluid observation and allowing for detection of biological and chemical molecules (Figure 1). In our previous study, we investigated LMs immersed into a liquid environment to boost their lifetime without compromising

their mechanical and physical properties, with precise temperature controllability for microreactor based applications.[40] Surprisingly, LMIL stabilized with a thinner coating layer, can render real-time UV and fluorescent spectrophotometric evaluation. To further investigate and leverage this distinctive function of LMILs, we demonstrated multi-planar real-time monitoring of yeast cell culture within the spatial stereoscopic construction along with chemical reaction-based methylene blue (MB) degradation reaction. We anticipate the real-time monitoring with cell activities and analysis of reaction kinetics will be of paramount importance in biotechnological and stoichiometric chemistry processes.

Results and discussion

The hydrophobic shells of LMs are an essential prerequisite offering structural integrity by restricting LMs from wetting the external solid surface and functional benefits by impeding the physical information interaction for optical transmissibility. McEleney et al reported the construction of particle shells on droplets by tailoring particle size and density,[41] and the results showed that even a fewer number of layer shell was expected to weaken the barrier of information transmission. Interestingly, in our previous study, LMs suspended in organic media showed similar constructed shell whose structural lifetime was pronounced and exhibited optical transparency.[40] In this study, we adapted a new approach wherein LMs were stabilized by superhydrophobic CDs/POSS nanoparticles (luminescent carbon dots were functionalized with polyhedral oligomeric silsesquioxane),.[11] The LM surface composed of yellowish CDs/POSS nanoparticles is still opaque in the air while transforming to ultra-high

transmission in a liquid environment (Figures 2a and 2b). We believe that the pronounced optical transmittance is due to tailored shell thickness and reduced agglomerated shell particles (Figures 2c and 2d). In addition, LMIL can be visualized using an oil immersion lens (Figure 2e); The optical transmissibility of HT-LMIL was investigated and compared to naked water droplet in liquid, and only in ultraviolet region, the transmittance gets reduced because of the CDs/POSS particles absorbance (Figure 2f). The inset verifies the transparent texture of water LMs in the organic reagent. Besides, an assortment of size particles generated transparent armors by HT-LMIL method (Figure S1), overcoming the particle size restriction of present transparent LMs, which can only be formed by monolayer silica nanoparticles. Taking the transparency of a water droplet in oil as a benchmark, the normalized dye intensity of LMILs coated by whether nanoscale or microscale PTFE particles reached up to 80%, doubling that of same LMs in the air (Figure 2g). That implies the HT-LMIL strategy could expand the LM applications in multifunctional scenarios by a generally applicable way.

LM-based cell culture can be regarded as a cell-compatible culture chamber compared to a bulk culture medium, owing to their structural advantage in mass and nutrient transfer.[15] Therefore, by manipulating the system stability and environment variability in our earlier study, a long-term incubation of yeast cells was constructed in a continuous and multi-spatial stereoscopic environment of LMIL. As shown in Figures 3a, the distribution of yeast cells in this 3D micro-environment can be directly visualized by layer-by-layer microscopic imaging. Observation of different cellular

behaviors such as penetration, migration, and adhesion within the culture medium can be clearly seen and traced in a high-throughput way within the 3D micro-environment and thereby diminishes the requirement of expensive 3D fluorescence microscopes. On the top layer, the dispersive cells were found to float in the culture medium rather than adhere to the aggregated particles (Figure 3b). A higher invasion of the suspended yeast cells can be readily captured from the middle plane of culture medium (Figures 3c and 3d) with significant cell-cell adhesion and stacking observed at the bottom of the LMIL occurring after 30 min of incubation (Figure 3e). Additionally, at the bottom of LMs interface, there was no contact between the yeast cells and hydrophobic particles, avoiding the ingestion of stabilizers by the cells.[38,42] .

Importantly, the viability of yeast cells in a HT-LMIL can also be continuously and qualitatively tested and analysed by an intuitive methylene blue (MB) labeling[43,44] using normal microscopes, avoiding complex post-processing and parallel design of an MTT (3-(4,5-dimethylthiazol-2-y-l)-2,5-diphenyltetrazolium bromide) assay. As shown in Figures S2 a-c, the number of dead cells (blue cells) had no obvious increase during 4 h incubation. The time-varying cell viability between 3D LMIL culture and 2D cell culture was also compared and shown in Figure S2d. Along with the incubation, the live cell percentage in HT-LMIL was higher than that in the 2D petri dish, not only proving the feasibility of real-time monitoring of cell viability in LMIL but also suggesting promising biocompatibility of the hydrophobic CDs/POSS shell and oil.[45,46]

Theoretically, compared to the naked sessile droplet on superhydrophobic surface or low moduli substrate (<1 kPa), it is believed that particle composed viscoelastic

coating and stiff substrate (> 10 kPa) could induce cell 3D aggregation and even differentiation in a "one-pot" LM. [38,47,48] To confirm the advantages of LM 3D culture strategy by directly visualizing the above dynamic interactions in the LM bioreactor, a transparent LMIL-based bioreactor was applied for tracking cellular morphodynamics and density evolution during the incubation process. Herein a 10 μL LMIL filled with culture medium was used to *in situ* monitor3D yeast proliferation. As shown in Figure 4a (i-vi), the yeast cells were stacked tightly as a bulk agglomeration and remained as a 3D bonded structure during the whole visualizing process. Specially, the budding reproduction of yeast cells in HT-LMIL was clearly recorded by a series of time-lapse images, as shown in Figure 4a iii and Figure S3. Statistically, both the individual cell size and agglomeration area increased firstly and then underwent a stationary phase, which is a signature feature of indicating the 3D aggregate formed in HT-LMIL possesses differentiation potential to diversify into functional cell subpopulations (Figure 4c).[49] Compared to the hanging drop technique, which only generates a single cellular spheroid, an LM can yield several spheroids once with high reproducibility.[12,42] As demonstrated in Figures 4d and Figure S4, the yeast cells initially distributed uniformly in LMIL. Then, more groups of cells aggregated simultaneously, heralding the formation of multiple spheroids in HT-LMIL. The evolution of total cell population in the LMIL was also consistent with the typical cell growth curve from an exponential growth phase to a stationary phase, proving the high viability of yeast cells in HT-LMIL (Figure 4e).[50]

In order to further assess the technological importance of the LMIL-based bioassay,

we investigated the dynamic cellular processes in HT-LMIL in a noninvasive manner by using Laser Scanning Confocal Microscopy (LSCM) technique.[51] Also, there is less work being conducted to long-term monitor the dynamic variation of cellular functions and structures due to technical limitations such as high toxicity, irreversible photobleaching, and low labeling precision of established fluorescent dyes.[52] In this work, emerging water-soluble N-doped luminescent carbon dots (N-CDs) with favorable stability and biocompatibility for photoluminescence (PL) bio-labeling[53] were dissolved in a culture medium containing the HT-LMIL with cultured cells for 30 min. As shown in Figures 5a-5c and S5, we observed the internalization of N-CDs, whose fluorescence intensity (FI) in the yeast cells was found to be dynamic along with gemmation, which in turn facilitated the vital cellular activity monitoring. We also observed a drastic cytoplasmic activity of the germinating cells which was marked by a decline in FI when compared to the newborn cells with more stable cell-wall (Figure 5d). It is also worth noting that the shell particles of CDs/ POSS could also emit fluorescence in solid state, but interestingly, N-CDs worked only in solution (Figure S7), which implied aggregation-induced quenching of N-CDs was weakened by cladding with POSS. The presented method diminishes the need for an animal model approach towards the evaluation of the efficacy of cell-based therapies. Furthermore, uniting the great transparency and high-temperature tolerance of HT-LMIL with fluorescent N-CDs probes is conducive to expand its accessible applications to the real-time quantitative polymerase chain reaction (qPCR) or other biochemical reactions.[54-56]

Optical spectroscopy is another commonly used quantitative method for process monitoring due to its sensitivity to molecular vibration and electronic state.[57] The as-developed LMIL-based microreactor provides multifaceted behavior of real-time observation for bioreaction as well as, *in situ* spectroscopic characterization of chemical lab-in-a-drop. Here, we demonstrated the methylene blue (MB) degradation reaction in a 10 μL LMIL drop, with UV-vis absorption spectrometry monitoring internal process (Figure 6a). Figure 6b shows a marked decline in the absorption peak at 665 nm implying the reduction of MB content. The overall degradation process of MB by $NaBH_4$ falls under a pseudo-first-order reaction and expressed as:

$$ln\left(C / C_0\right) = -k_{app}t \quad (1)$$

where k_{app} and t refer to reaction rate constant and time, respectively. As shown in Figure 6c, a strong linear relationship between $-\ln(C/C_0)$ and time indicates the feasibility of an LMIL-based *in situ* characterization platform with a color transition of inserts demonstrating the applicability of HT-LMIL as a microreactor, which is a unique characteristic of this system. Specifically, Figure 6d reveals the instantaneous MB detailed information during the reaction process, with much shorter characterization intervals (5s) adopted, suggesting the promising transparency triggered high detection sensitivity of LMIL-based reactors. Notably, there is a distinct difference between k_1 (k_{app} for Figure 6b) and k_2 (k_{app} for Figure 6d) from the fitted pseudo-first-order reaction, which may be caused by an unevenly distributed concentration.

Conclusion

In summary, we have demonstrated the potential of LMIL-based transparent

micro-bioreactor as a feasible platform for real-time microscopic observation. The interfacial re-configurability of LMIL is achieved by altering the density of hydrophobic shell particles which surround LMs with comparable transmittance like a naked water droplet. This mechanism is in favor of transforming LMs coated by diverse particles into perspective LMIL. An *in situ* visualization and real-time optical spectroscopic characterization of the HT-LMIL enables the observation of entire process of yeast cell culturing on a dynamic scale. The high cell viability of HT-LMIL maintained in time-varying process, imposing no toxicity of liquid-liquid interface and coating particles to the whole system. Combined with its extended lifetime and precise control of the environmental reaction conditions, HT-LMIL creates a strong paradigm shift for *in- situ* observation of cell proliferation and 3D cellular spheroids development. Similarly, confocal microscopic studies as the HT-LMIL's *in situ* monitoring platform gave an in-depth understanding of cell vital actability upon labeling with fluorescent carbon dots. Finally, a real-time transition information of methylene blue degradation also added another key character to our system. This novel study provides a unique and yet beneficial development of LMIL-based microscopic characterization as a versatile and feasible platform to be applied for a high-throughput real-time micro/bio-reactor, chemical analysis and process monitoring and warrants interest in the arena of bioengineering and analytical/physical chemistry.

Acknowledgement

We are grateful for final support from National Key Research and Development

Program of China (2021YFC3001602). This research was also financially supported by grants 9610469 and 7005636 from the City University of Hong Kong.

Experimental section

Materials

N-doped carbon dots (N-CDs, average size is 2.5 nm) and hydrophobic N-CD modified by POSS (CDs/POSS, average size is 6.6 nm) were prepared according to our previous work[39].[11] The silica nanoparticles (2-40 nm) and different size PTFE particles (100-500 nm, 1-3 μm, and 12 μm) were purchased from SuYuan Chemical Co., Ltd (Dongguan, China). Methylene blue (MB) dye was purchased from Aladdin Chemical Co., Ltd (Shanghai, China). All the chemicals were used as received without further purification. Deionized water (DI water) prepared by a Hitech Laboratory Water Purification System DW100 (Shanhai Hitech Instruments Co. Ltd), was used for all experiments.

Generation of transparent liquid marbles in liquid.

The LMs were fabricated by classical shaking-rolling method. Firstly, 10 μL DI water dyed by MB (0.1 mg· mL^{-1}) was rolled onto a bed of hydrophobic CDs/POSS particles, rendering the nanoparticles to attach at the liquid-air interface forming LMs. The constructed LMs were then transferred into octadecene to generate liquid marbles in liquid (LMIL). With a gentle shaking of LMIL, the transparent appearance was obtained. The LMIL coated by silica nanoparticles and different size PTFE particles were synthesized by same method. Their digital images were captured by a digital camera (Basler, ace acA1300-200um) equipped with a telecentric lens (Edmund Optics, Compact TL). The MB dye intensity of each sample in the air and in the oil was measured by Image J in triplicate to report the mean values.

Assessment of proliferation property of Yeast cells

0.1mg • mL^{-1} dry yeast inoculum was cultured in 10 μL of LM along with 5 wt% glucose solution and transferred into octadecene. After few minutes, the LMIL was observed by an optical microscope for real-time morphological and functional studies at room temperature (26 ℃). The diameter of cells and area of cell aggregations were measured in triplicate by Image J every 50 minutes. Their mean values were calculated and plot with time.

Yeast cell viability test

The viability of yeast cells cultured in HT-LMIL bioreactor and 2D petri dish was tested by MB labeling with an optical microscope. Firstly, same density of cells were cultured in a HT-LMIL and a petri dish, respectively .Then, their culture mediums were treated by MB (0.1 mg • mL^{-1}) for 10 mins, respectively. Samples were imaged at three different regions every hour. Their live cell number and total cell number in each image were counted and averaged. The comparison of cell viability percentage between 3D LMIL and 2D petri dish was expressed as:

$$Cell\ viability = \frac{Live\ cell\ muber_{LMIL}/Total\ cell\ number_{LMIL}}{Live\ cell\ number_{2D\ petri\ dish}/Total\ cell\ number_{2D\ petri\ dish}} \times 100\% \ .$$

***In situ* monitoring by laser scanning confocal microscopy (LSCM)**

Likely, 10 μL LMIL containing 0.1 mg • mL^{-1} dry yeast and 5 wt% glucose solution was cultured at room temperature, then fluorescent N-CDs were added into the media. LSCM (TCS SP8, Leica, Germany; excited by 405 nm laser) was employed for the fluorescent visualization of cell vital activities.

Methylene blue degradation evaluation using UV-Vis spectroscopic method

10 μL of LMIL solution containing MB (0.1 mg • mL^{-1}) and $NaBH_4$ (1 mg • mL^{-1})

was directly transferred to UV-vis photo spectrometer (200 - 800 nm), and irradiated with UV-vis light to study the catalytic efficiency of the system.

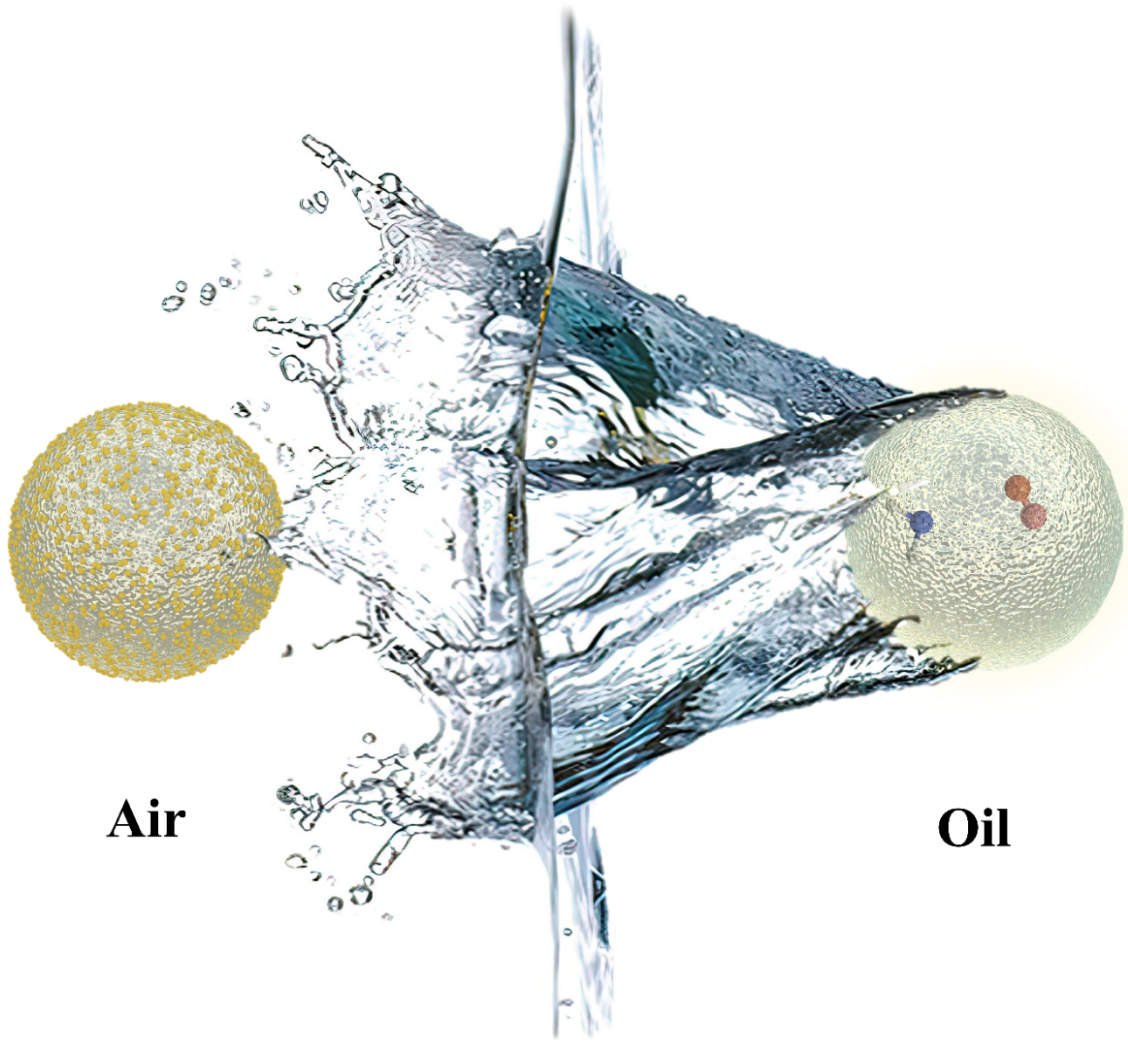

Figure 1. Schematic illustration of highly transparent Liquid marble in liquid (HT-LMIL) microreactor for biological and chemical applications. **Left:** traditional liquid marbles in air (with low transparency); **right:** HT-LMIL with ultra-high transparency

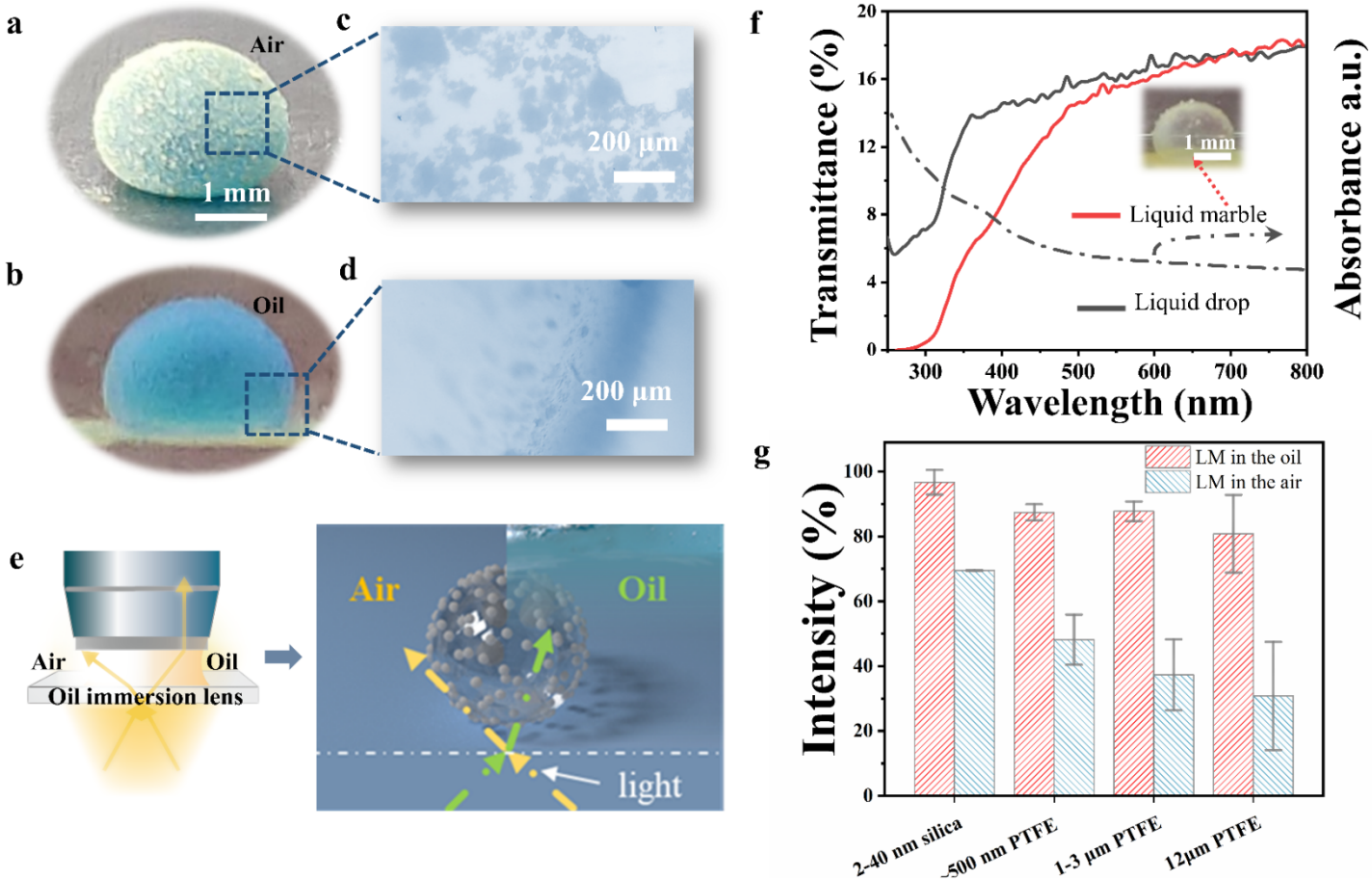

Figure 2. (a) Schematic diagram of transparency shift between LMs and HT-LMIL; Optical images of (a) 10 μL LMs and (b)10 μL LMIL dyed with methylene blue (MB), respectively; Superficial particles of (c) LMs and (d) LMIL; (e) Operating principle of oil immersion lens for HT-LMIL; (f) Transmittances between LMIL and water drop in liquid. (g) Normalized MB dye intensity percentage of LMs coated by different particles in the air and in the oil. The benchmark is the dye intensity of water droplet in the oil.

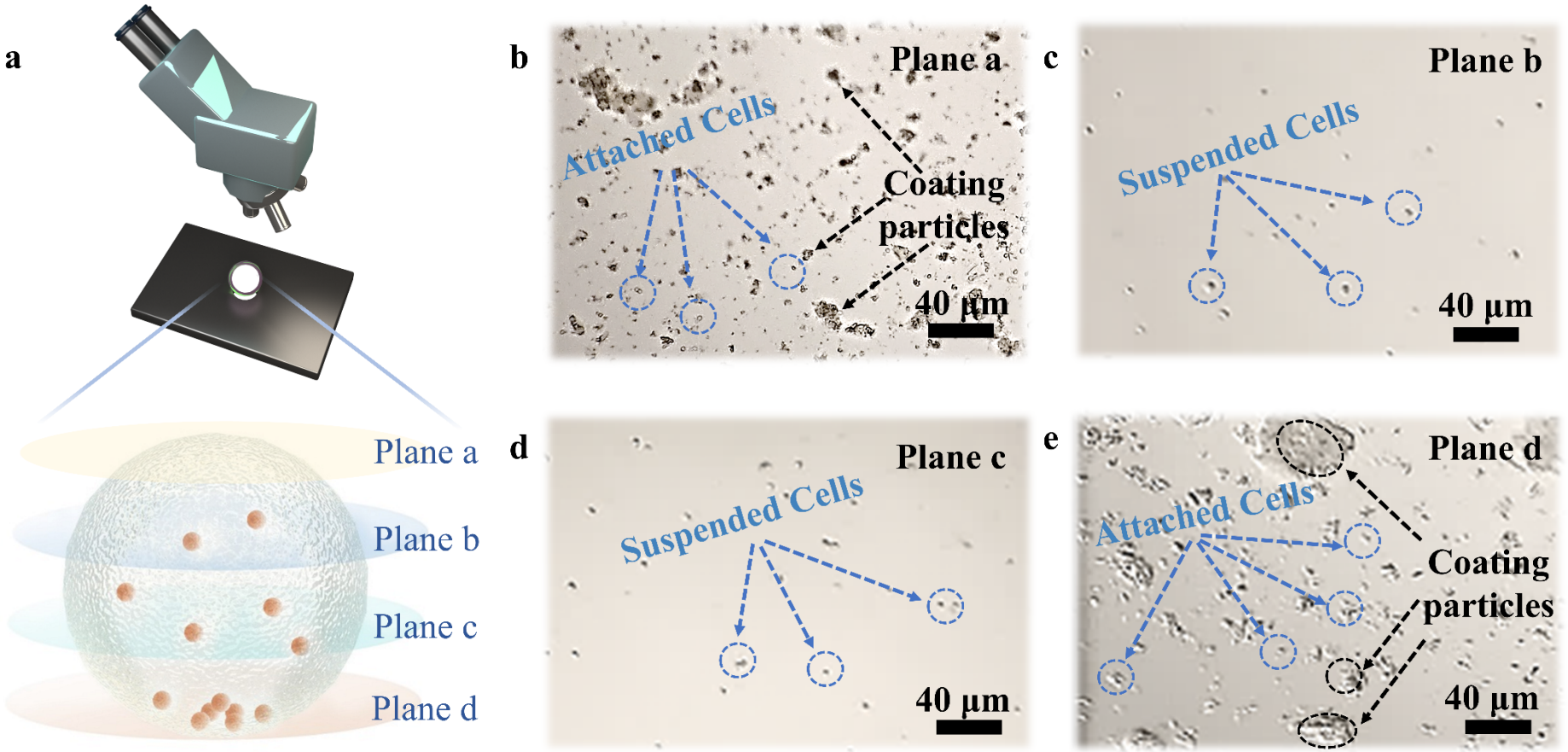

Figure 3. (a) Schematic diagram of layer-by-layer observation of 3D cell culturing in HT-LMIL; Microimaging of yeast cell from (b) plane a (top), (c) plane b (middle 1), (d) plane c (middle 2), and (e) plane d (bottom).

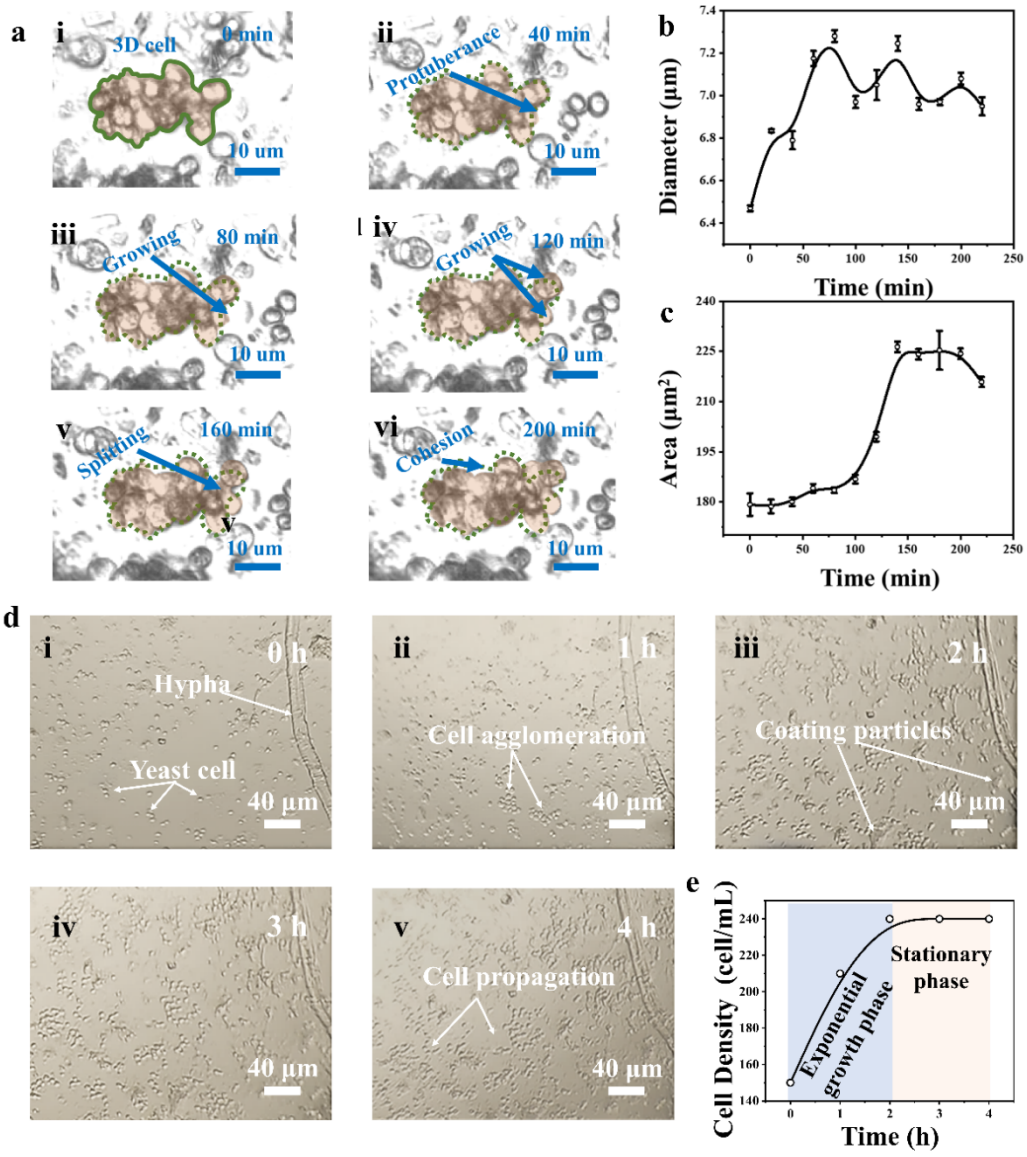

Figure 4. Cellular morphodynamics analysis in HT-LMIL. (a) The dotted line and brown shaded area refer to the initial outline and real-time shape of bulk cells observed at (i) 0 min, (ii) 40 min, (iii) 80 min, (iv) 120 min, (v) 160 min and (vi) 200 min. (b) Cell diameters growth over culture time. (c) Area changes of 3D cell agglomeration over time. (d) Propagation process of yeast in LMIL (i) 0 h, (ii) 1 h, (iii) 2 h, (iv) 3 h and (v) 4 h. (e) Quantitative amount growth of yeast in HT-LMIL.

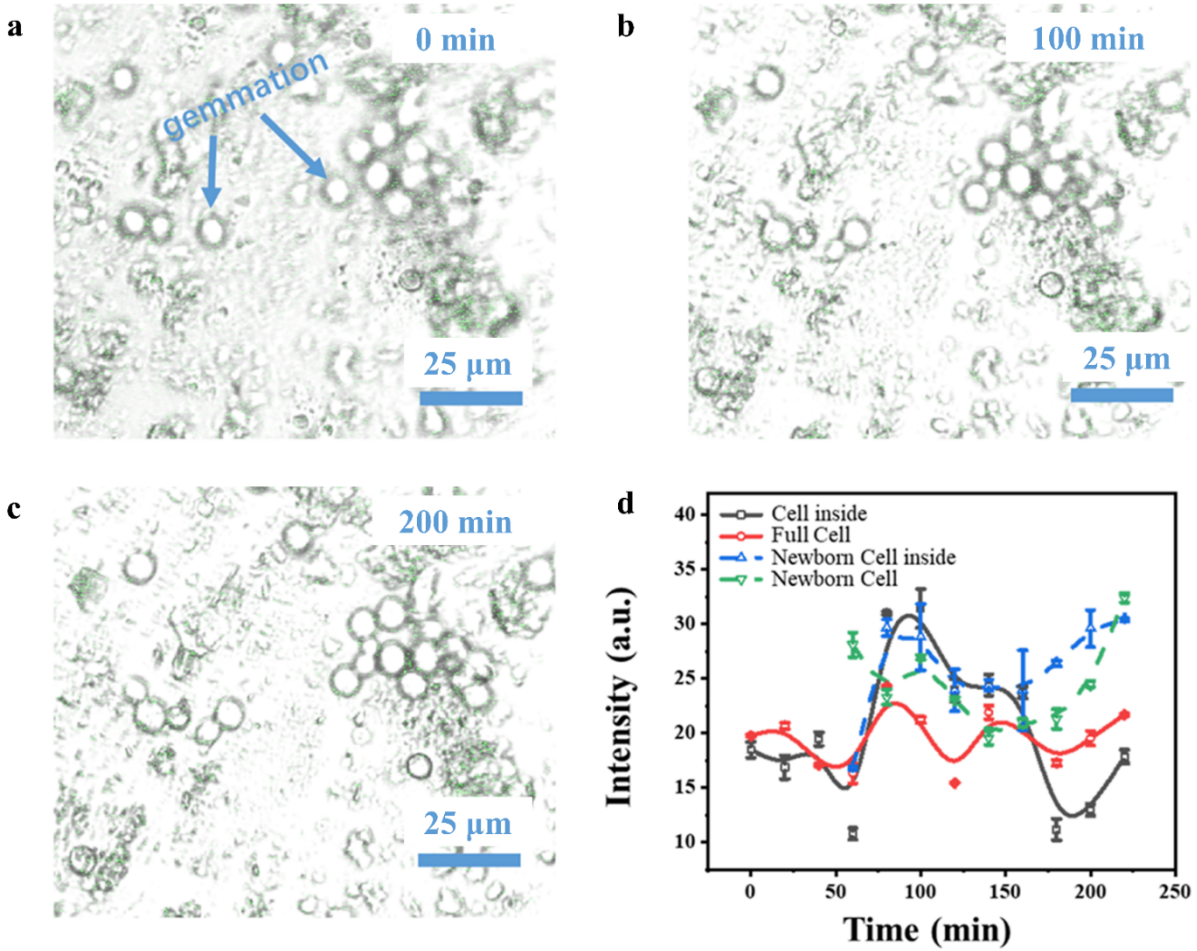

Figure 5. Confocal monitoring of cell proliferation process labeled by N-CDs probes in HT-LMIL: (a) 0 min, (b) 100 min, (c) 200 min, (d) Photoluminescence (PL) spectra of the individual living cell. Cell inside and full cell indicate PL intensity measurements without and with the cell wall, respectively.

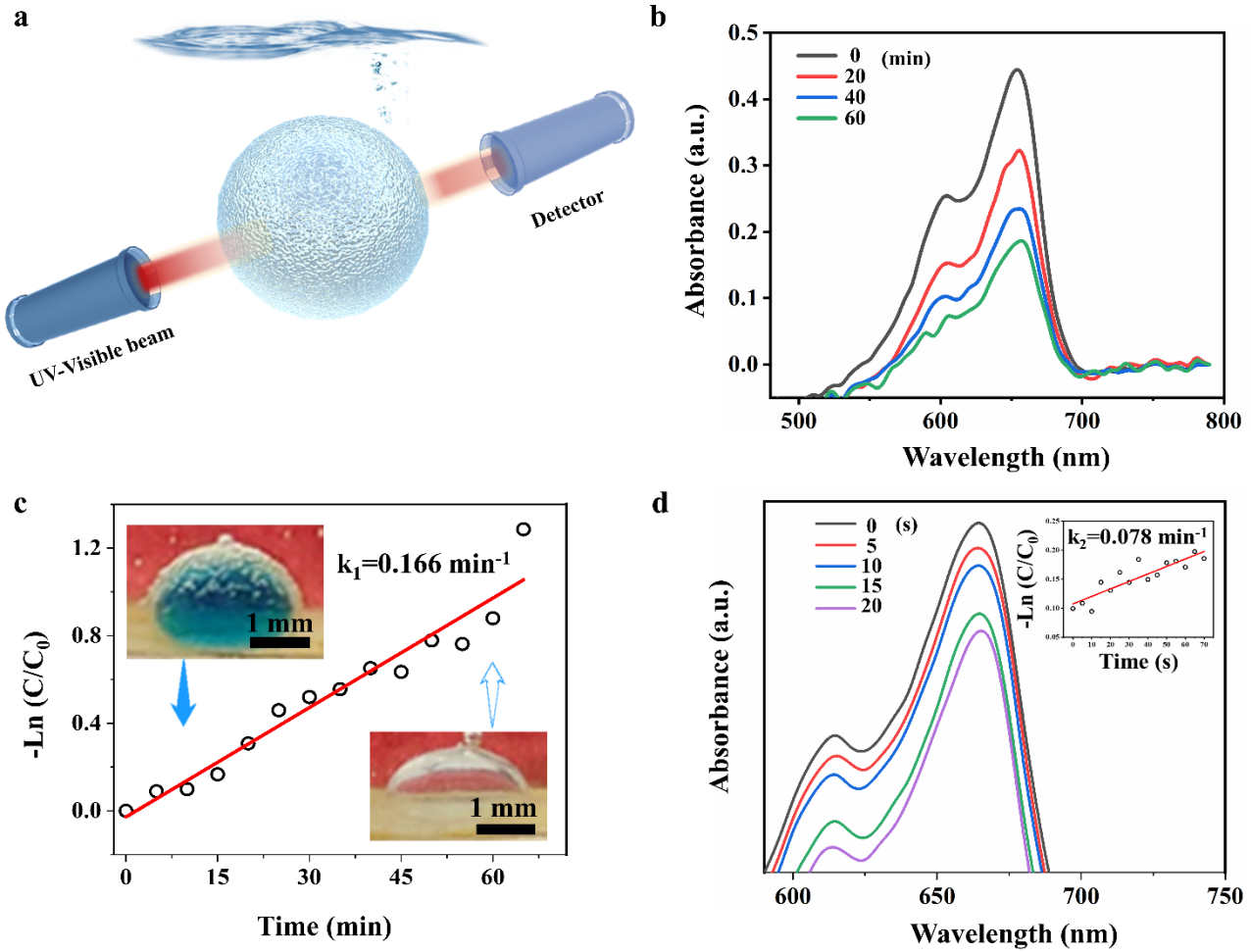

Figure 6. (a) Schematic diagram of spectrum detection of methylene blue (MB) degradation in HT-LMIL; (b) UV-vis absorption changes of MB dye solution degradation in LMIL under 60 min irradiation. (c) The plot of ln(C/C0) as a function of time with pseudo-first-order fitting. k_1 is the reaction rate constant. The insets are optical images of MB degradation degree in 10 μL HT-LMIL at 10 min and 60 min, respectively. (d) UV-vis absorption changes of MB dye solution degradation in HT-LMIL over the shortest interval of irradiation time.

References

(1) Aussillous, P.; Quéré, D., Liquid marbles. *Nature* **2001,** *411* (6840), 924-927.
(2) Zhu, R.; Liu, M.; Hou, Y.; Zhang, L.; Li, M.; Wang, D.; Fu, S., One-Pot Preparation of Fluorine-Free Magnetic Superhydrophobic Particles for Controllable Liquid Marbles and Robust Multifunctional Coatings. *ACS Appl. Mater. Interfaces* **2020,** *12* (14), 17004-17017.
(3) Bormashenko, E., Liquid Marbles, Elastic Nonstick Droplets: From Minireactors to Self-Propulsion. *Langmuir* **2017,** *33* (3), 663-669.
(4) Fullarton, C.; Draper, T. C.; Phillips, N.; Mayne, R.; de Lacy Costello, B. P. J.; Adamatzky, A., Evaporation, Lifetime, and Robustness Studies of Liquid Marbles for Collision-Based Computing. *Langmuir* **2018,** *34* (7), 2573-2580.
(5) Chu, Y.; Wang, Z.; Pan, Q., Constructing Robust Liquid Marbles for Miniaturized Synthesis of Graphene/Ag Nanocomposite. *ACS Appl. Mater. Interfaces* **2014,** *6* (11), 8378-8386.
(6) Sheng, Y.; Sun, G.; Wu, J.; Ma, G.; Ngai, T., Silica-Based Liquid Marbles as Microreactors for the Silver Mirror Reaction. *Angew. Chem., Int. Ed.* **2015,** *54* (24), 7012-7017.
(7) Han, X.; Lee, H. K.; Lee, Y. H.; Ling, X. Y., Dynamic Rotating Liquid Marble for Directional and Enhanced Mass Transportation in Three-Dimensional Microliter Droplets. *J. Phys. Chem. Lett* **2017,** *8* (1), 243-249.
(8) deMello, A. J., Control and detection of chemical reactions in microfluidic systems. *Nature* **2006,** *442* (7101), 394-402.
(9) Qin, S.; Wang, D.; Wang, J.-X.; Pu, Y.; Chen, J.-F., Polyhedral oligomeric silsesquioxane-coated nanodiamonds for multifunctional applications. *J. Mater. Sci.* **2018,** *53* (23), 15915-15926.
(10) Liu, Z.; Yang, T.; Huang, Y.; Liu, Y.; Chen, L.; Deng, L.; Shum, H. C.; Kong, T., Electrocontrolled Liquid Marbles for Rapid Miniaturized Organic Reactions. *Adv. Funct. Mater.* **2019,** *29* (19), 1901101.
(11) Zhao, Z.; Qin, S.; Wang, D.; Pu, Y.; Wang, J.-X.; Saczek, J.; Harvey, A.; Ling, C.; Wang, S.; Chen, J.-F., Multi-stimuli-responsive liquid marbles stabilized by superhydrophobic luminescent carbon dots for miniature reactors. *Chem. Eng. J.* **2020,** *391*, 123478.
(12) Chen, M.; Shah, M. P.; Shelper, T. B.; Nazareth, L.; Barker, M.; Tello Velasquez, J.; Ekberg, J. A. K.; Vial, M.-L.; St John, J. A., Naked Liquid Marbles: A Robust Three-Dimensional Low-Volume Cell-Culturing System. *ACS Appl. Mater. Interfaces* **2019,** *11* (10), 9814-9823.
(13) Wang, B.; Liu, Y.; Zhang, Y.; Guo, Z.; Zhang, H.; Xin, J. H.; Zhang, L., Bioinspired Superhydrophobic Fe3O4@Polydopamine@Ag Hybrid Nanoparticles for Liquid Marble and Oil Spill. *Adv. Mater. Interfaces* **2015,** *2* (13), 1500234.
(14) Anyfantakis, M.; Jampani, V. S. R.; Kizhakidathazhath, R.; Binks, B. P.; Lagerwall, J. P. F., Responsive Photonic Liquid Marbles. *Angew. Chem., Int. Ed.* **2020,** *59* (43), 19260-19267.
(15) Wang, B.; Chan, K. F.; Ji, F.; Wang, Q.; Chiu, P. W. Y.; Guo, Z.; Zhang, L.,

On-Demand Coalescence and Splitting of Liquid Marbles and Their Bioapplications. *Adv. Sci. (Weinheim, Ger.)* **2019,** *6* (10), 1802033.
(16) Chandan, S.; Ramakrishna, S.; Sunitha, K.; Chandran, M. S.; Kumar, K. S. S.; Mathew, D., pH-responsive superomniphobic nanoparticles as versatile candidates for encapsulating adhesive liquid marbles. *J. Mater. Chem. A* **2017,** *5* (43), 22813-22823.
(17) Paven, M.; Mayama, H.; Sekido, T.; Butt, H.-J.; Nakamura, Y.; Fujii, S., Light-Driven Delivery and Release of Materials Using Liquid Marbles. *Adv. Funct. Mater.* **2016,** *26* (19), 3199-3206.
(18) Kavokine, N.; Anyfantakis, M.; Morel, M.; Rudiuk, S.; Bickel, T.; Baigl, D., Light-Driven Transport of a Liquid Marble with and against Surface Flows. *Angew. Chem., Int. Ed.* **2016,** *55* (37), 11183-11187.
(19) Wang, D.; Zhu, L.; Chen, J.-F.; Dai, L., Liquid Marbles Based on Magnetic Upconversion Nanoparticles as Magnetically and Optically Responsive Miniature Reactors for Photocatalysis and Photodynamic Therapy. *Angew. Chem., Int. Ed.* **2016,** *55* (36), 10795-10799.
(20) Liu, Z.; Fu, X.; Binks, B. P.; Shum, H. C., Coalescence of electrically charged liquid marbles. *Soft Matter* **2017,** *13* (1), 119-124.
(21) Fujii, S.; Yusa, S.-i.; Nakamura, Y., Stimuli-Responsive Liquid Marbles: Controlling Structure, Shape, Stability, and Motion. *Adv. Funct. Mater.* **2016,** *26* (40), 7206-7223.
(22) Shang, Q.; Hu, L.; Hu, Y.; Liu, C.; Zhou, Y., Fabrication of superhydrophobic fluorinated silica nanoparticles for multifunctional liquid marbles. *Applied Physics A* **2017,** *124* (1), 25.
(23) Arbatan, T.; Li, L.; Tian, J.; Shen, W., Liquid Marbles as Micro-bioreactors for Rapid Blood Typing. *Adv. Healthcare Mater.* **2012,** *1* (1), 80-83.
(24) Gao, W.; Lee, H. K.; Hobley, J.; Liu, T.; Phang, I. Y.; Ling, X. Y., Graphene Liquid Marbles as Photothermal Miniature Reactors for Reaction Kinetics Modulation. *Angew. Chem., Int. Ed.* **2015,** *54* (13), 3993-3996.
(25) Han, X.; Koh, C. S. L.; Lee, H. K.; Chew, W. S.; Ling, X. Y., Microchemical Plant in a Liquid Droplet: Plasmonic Liquid Marble for Sequential Reactions and Attomole Detection of Toxin at Microliter Scale. *ACS Appl. Mater. Interfaces* **2017,** *9* (45), 39635-39640.
(26) Avrămescu, R.-E.; Ghica, M.-V.; Dinu-Pîrvu, C.; Udeanu, D. I.; Popa, L., Liquid Marbles: From Industrial to Medical Applications. *Molecules (Basel, Switzerland)* **2018,** *23* (5), 1120.
(27) Xue, Y.; Wang, H.; Zhao, Y.; Dai, L.; Feng, L.; Wang, X.; Lin, T., Magnetic Liquid Marbles: A "Precise" Miniature Reactor. *Adv. Mater.* **2010,** *22* (43), 4814-4818.
(28) Oliveira, N. M.; Reis, R. L.; Mano, J. F., The Potential of Liquid Marbles for Biomedical Applications: A Critical Review. *Adv. Healthcare Mater.* **2017,** *6* (19), 1700192.
(29) Aalders, J.; Léger, L.; Tuerlings, T.; Ledda, S.; van Hengel, J., Liquid marble technology to create cost-effective 3D cardiospheres as a platform for in vitro drug testing and disease modelling. *MethodsX* **2020,** *7*, 101065.

(30) Aberle, C.; Lewis, M.; Yu, G.; Lei, N.; Xu, J., Liquid marbles as thermally robust droplets: coating-assisted Leidenfrost-like effect. *Soft Matter* **2011,** *7* (24), 11314-11318.
(31) Pitois, O.; Rouyer, F., Rheology of particulate rafts, films, and foams. *Curr. Opin. Colloid Interface Sci.* **2019,** *43*, 125-137.
(32) Luo, X.; Yin, H.; Li, X. e.; Su, X.; Feng, Y., CO2-Triggered microreactions in liquid marbles. *Chem. Commun. (Cambridge, U. K.)* **2018,** *54* (66), 9119-9122.
(33) Liu, Z.; Zhang, Y.; Chen, C.; Yang, T.; Wang, J.; Guo, L.; Liu, P.; Kong, T., Larger Stabilizing Particles Make Stronger Liquid Marble. *Small* **2019,** *15* (3), 1804549.
(34) Vialetto, J.; Hayakawa, M.; Kavokine, N.; Takinoue, M.; Varanakkottu, S. N.; Rudiuk, S.; Anyfantakis, M.; Morel, M.; Baigl, D., Magnetic Actuation of Drops and Liquid Marbles Using a Deformable Paramagnetic Liquid Substrate. *Angew. Chem., Int. Ed.* **2017,** *56* (52), 16565-16570.
(35) Huang, S.; Zhang, Y.; Shi, J.; Huang, W., Superhydrophobic Particles Derived from Nature-Inspired Polyphenol Chemistry for Liquid Marble Formation and Oil Spills Treatment. *ACS Sustainable Chem. Eng.* **2016,** *4* (3), 676-681.
(36) Bhosale, P. S.; Panchagnula, M. V.; Stretz, H. A., Mechanically robust nanoparticle stabilized transparent liquid marbles. *Appl. Phys. Lett.* **2008,** *93* (3), 034109.
(37) Nguyen, N.-K.; Singha, P.; Zhang, J.; Phan, H.-P.; Nguyen, N.-T.; Ooi, C. H., Digital Imaging-based Colourimetry for Enzymatic Processes in Transparent Liquid Marbles. *ChemPhysChem* **2021,** *22* (1), 99-105.
(38) Lin, K.; Chen, R.; Zhang, L.; Zang, D.; Geng, X.; Shen, W., Transparent Bioreactors Based on Nanoparticle-Coated Liquid Marbles for in Situ Observation of Suspending Embryonic Body Formation and Differentiation. *ACS Appl. Mater. Interfaces* **2019,** *11* (9), 8789-8796.
(39) XiaoguangLi; YiqiWang; JunchaoHuang; YaoYang; RenxianWang; XingguoGeng; DuyangZang, Monolayer nanoparticle-covered liquid marbles derived from a sol-gel coating. *Appl. Phys. Lett.* **2017,** *111* (26), 261604.
(40) Zhao, Z.; Ling, C.; Wang, D.; Wang, J.-X.; Saczek, J.; Pramana, S.; Sridhar, S.; Shang, J.; Xu, B. B.; Tsang, D. C. W.; Chen, J.-F.; Wang, S., Liquid Marbles in Liquid. *Small* **2020,** *16* (37), 2002802.
(41) McEleney, P.; Walker, G. M.; Larmour, I. A.; Bell, S. E. J., Liquid marble formation using hydrophobic powders. *Chem. Eng. J.* **2009,** *147* (2), 373-382.
(42) Sarvi, F.; Arbatan, T.; Chan, P. P. Y.; Shen, W., A novel technique for the formation of embryoid bodies inside liquid marbles. *RSC Adv.* **2013,** *3* (34), 14501-14508.
(43) Feizi, A.; Zhang, Y.; Greenbaum, A.; Guziak, A.; Luong, M.; Chan, R. Y. L.; Berg, B.; Ozkan, H.; Luo, W.; Wu, M.; Wu, Y.; Ozcan, A., Rapid, portable and cost-effective yeast cell viability and concentration analysis using lensfree on-chip microscopy and machine learning. *Lab on a Chip* **2016,** *16* (22), 4350-4358.
(44) Belak, Z. R.; Harkness, T.; Eskiw, C. H., A rapid, high-throughput method for determining chronological lifespan in budding yeast. *J Biol Methods* **2018,** *5* (4),

e106-e106.
(45) van Tatenhove-Pel, R. J.; Zwering, E.; Boreel, D. F.; Falk, M.; van Heerden, J. H.; Kes, M. B. M. J.; Kranenburg, C. I.; Botman, D.; Teusink, B.; Bachmann, H., Serial propagation in water-in-oil emulsions selects for Saccharomyces cerevisiae strains with a reduced cell size or an increased biomass yield on glucose. *Metab. Eng.* **2021,** *64*, 1-14.
(46) Loman-Cortes, P.; Binte Huq, T.; Vivero-Escoto, J. L., Use of Polyhedral Oligomeric Silsesquioxane (POSS) in Drug Delivery, Photodynamic Therapy and Bioimaging. *Molecules* **2021,** *26* (21), 6453.
(47) Zang, D. Y.; Rio, E.; Langevin, D.; Wei, B.; Binks, B. P., Viscoelastic properties of silica nanoparticle monolayers at the air-water interface. *Eur. Phys. J. E* **2010,** *31* (2), 125-134.
(48) Saha, K.; Keung, A. J.; Irwin, E. F.; Li, Y.; Little, L.; Schaffer, D. V.; Healy, K. E., Substrate Modulus Directs Neural Stem Cell Behavior. *Biophys. J.* **2008,** *95* (9), 4426-4438.
(49) Palková, Z.; Váchová, L., Yeast cell differentiation: Lessons from pathogenic and non-pathogenic yeasts. *Semin. Cell Dev. Biol.* **2016,** *57*, 110-119.
(50) Jäger, T.; Scherr, C.; Wolf, U.; Simon, M.; Heusser, P.; Baumgartner, S., Investigation of arsenic-stressed yeast (Saccharomyces cerevisiae) as a bioassay in homeopathic basic research. *Sci. World J.* **2011,** *11*, 568-583.
(51) Sarvi, F.; Jain, K.; Arbatan, T.; Verma, P. J.; Hourigan, K.; Thompson, M. C.; Shen, W.; Chan, P. P. Y., Cardiogenesis of Embryonic Stem Cells with Liquid Marble Micro-Bioreactor. *Adv. Healthcare Mater.* **2015,** *4* (1), 77-86.
(52) Unnikrishnan, B.; Wu, R.-S.; Wei, S.-C.; Huang, C.-C.; Chang, H.-T., Fluorescent Carbon Dots for Selective Labeling of Subcellular Organelles. *ACS Omega* **2020,** *5* (20), 11248-11261.
(53) Sharma, A.; Panwar, V.; Chopra, V.; Thomas, J.; Kaushik, S.; Ghosh, D., Interaction of Carbon Dots with Endothelial Cells: Implications for Biomedical Applications. *ACS Appl. Nano Mater.* **2019,** *2* (9), 5483-5491.
(54) Sreejith, K. R.; Gorgannezhad, L.; Jin, J.; Ooi, C. H.; Stratton, H.; Dao, D. V.; Nguyen, N.-T., Liquid marbles as biochemical reactors for the polymerase chain reaction. *Lab on a Chip* **2019,** *19* (19), 3220-3227.
(55) Sreejith, K. R.; Ooi, C. H.; Dao, D. V.; Nguyen, N.-T., Evaporation dynamics of liquid marbles at elevated temperatures. *RSC Adv.* **2018,** *8* (28), 15436-15443.
(56) Belza, J.; Opletalová, A.; Poláková, K., Carbon dots for virus detection and therapy. *Microchim. Acta* **2021,** *188* (12), 430.
(57) Pinterić, M.; Roh, S.; Uykur, E.; Hansen, N. H.; Pflaum, J.; Stolte, M.; Würthner, F.; Dressel, M., Trapped Exciton and Large Birefringence in Cl2–NDI Revealed by Optical Spectroscopy. *J. Phys. Chem. C* **2020,** *124* (32), 17829-17835.

Supporting Information

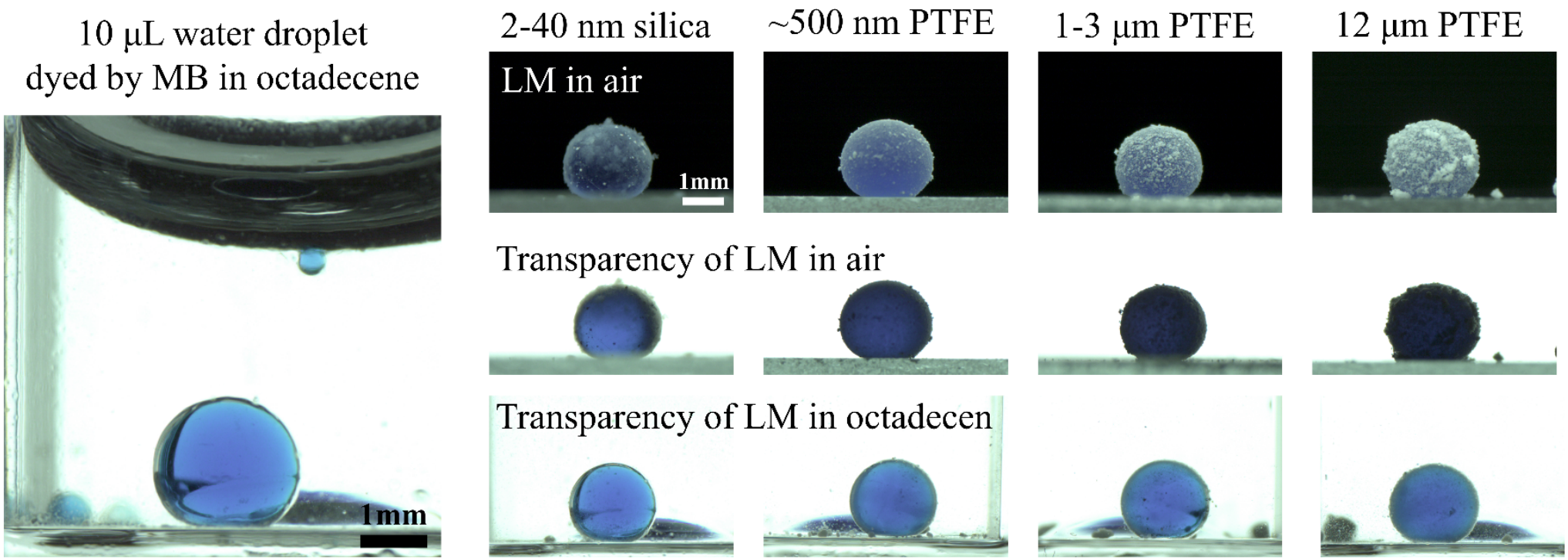

Figure S1. Optical pictures of 10 μ L LMIL with methylene blue dye coated by particles with different sizes in the air and in the oil, respectively.

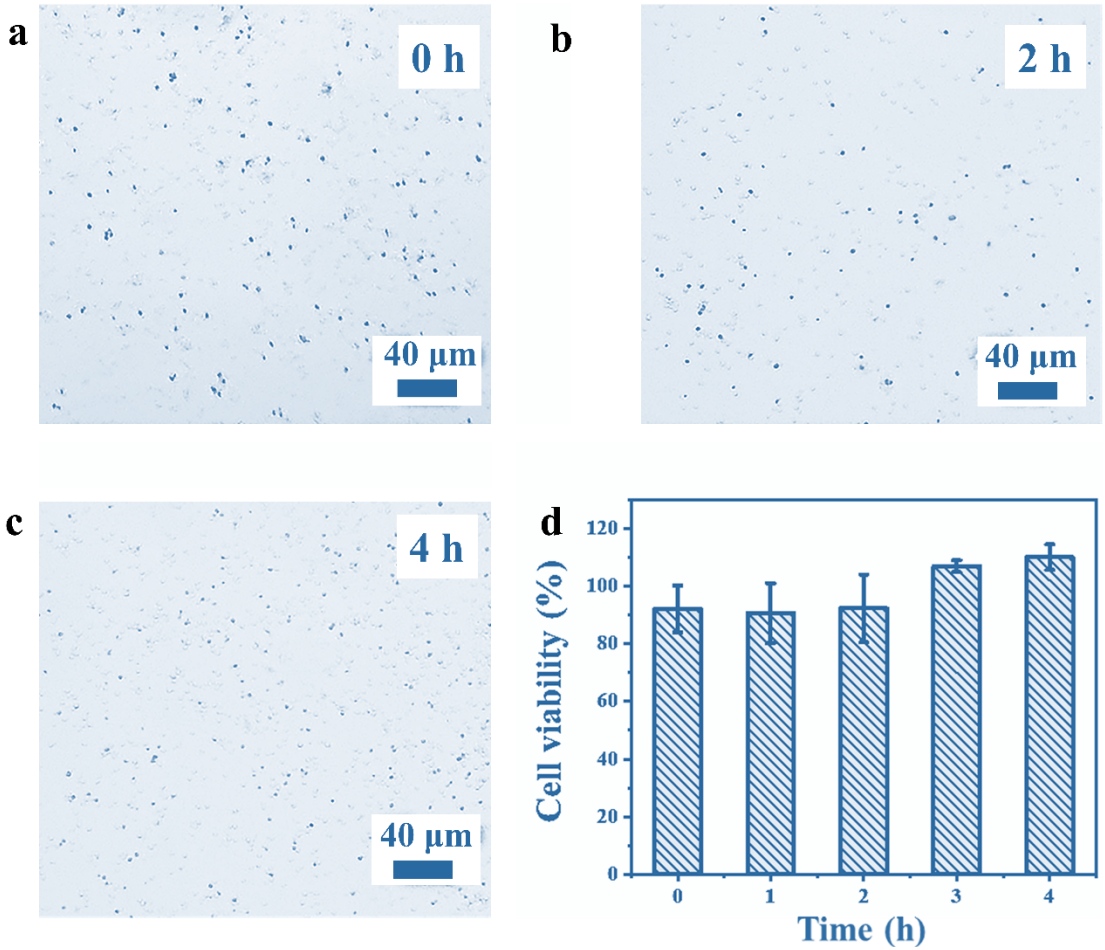

Figure S2. Cell viability of yeast cells cultured under different incubation time in LMIL: (a) 0h. (b) 2h. (c) 4h. Using the methylene blue labeling, dead cells were dyed with blue color. (d) Quantitative comparison of cell viability cultured by LMIL and 2D petri dish.

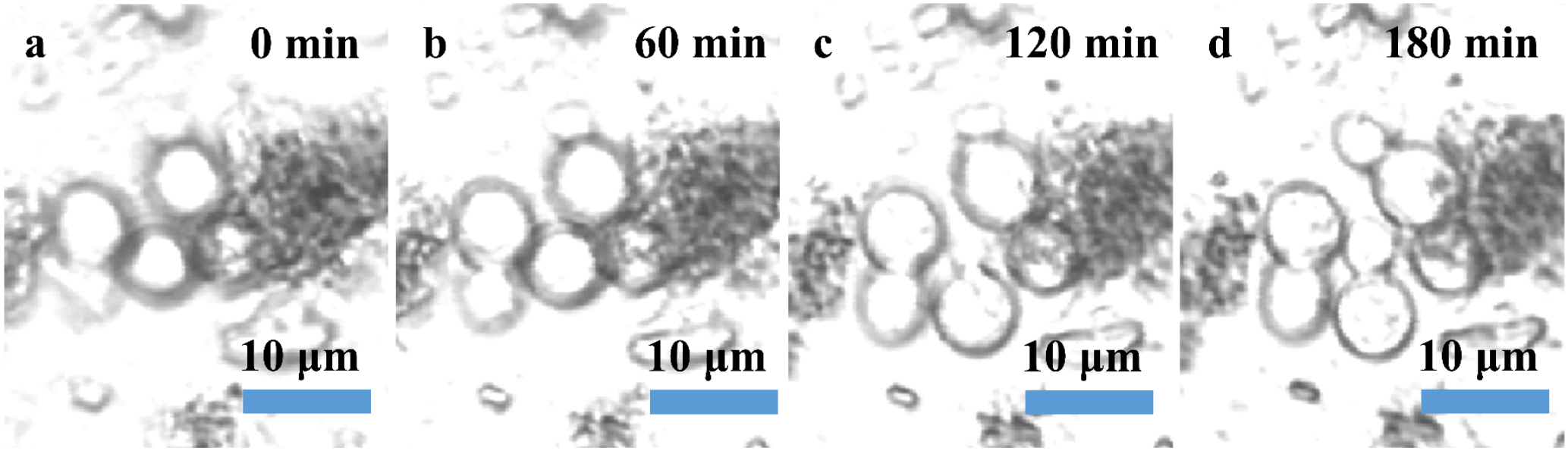

Figure S3. Budding reproduction process of yeast cells in LMIL. (a) 0 min, (b) 60 min, (c) 120 min, (d) 180 min.

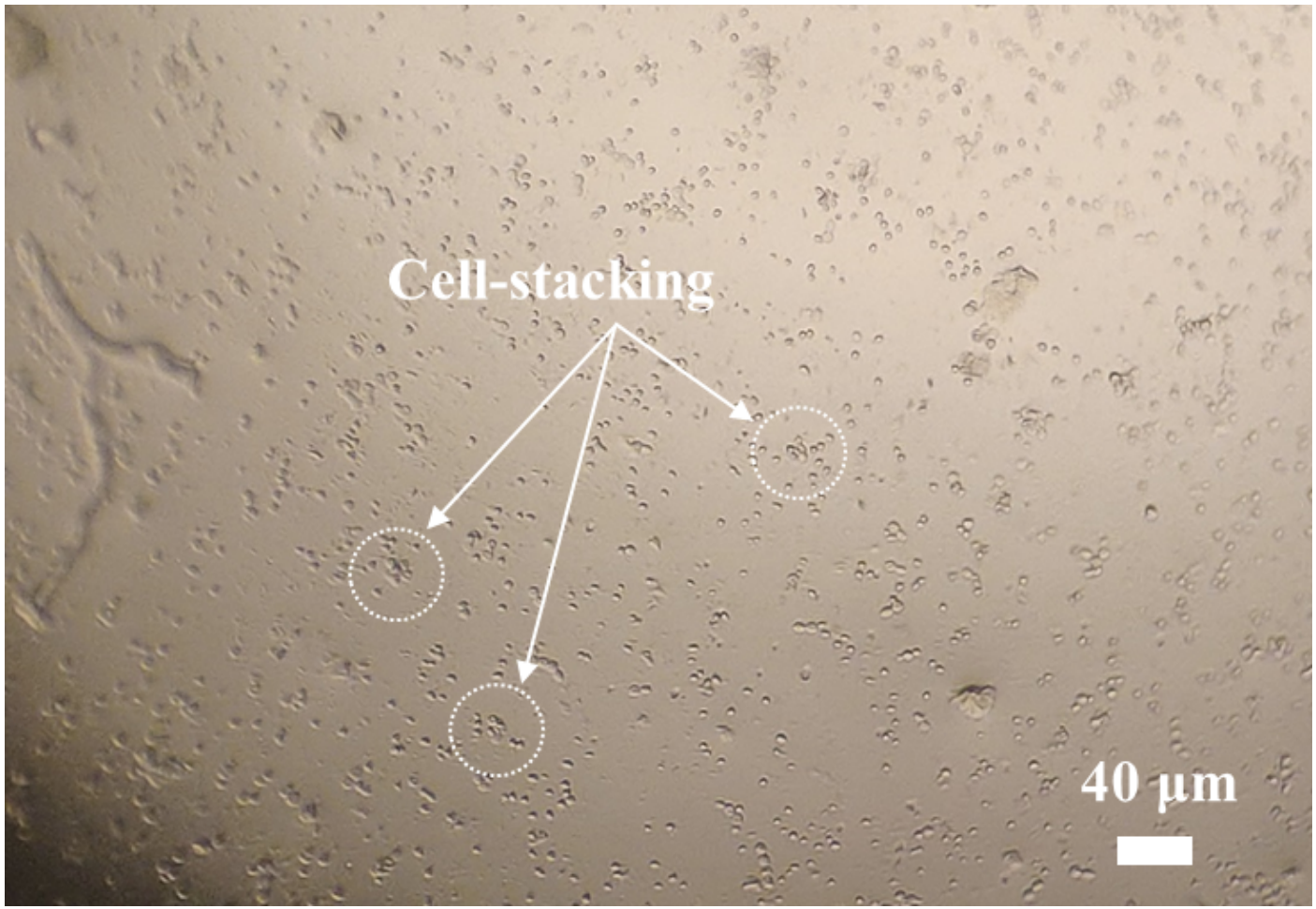

Figure S4. The aggregation behavior of yeast cells cultured in LMIL.

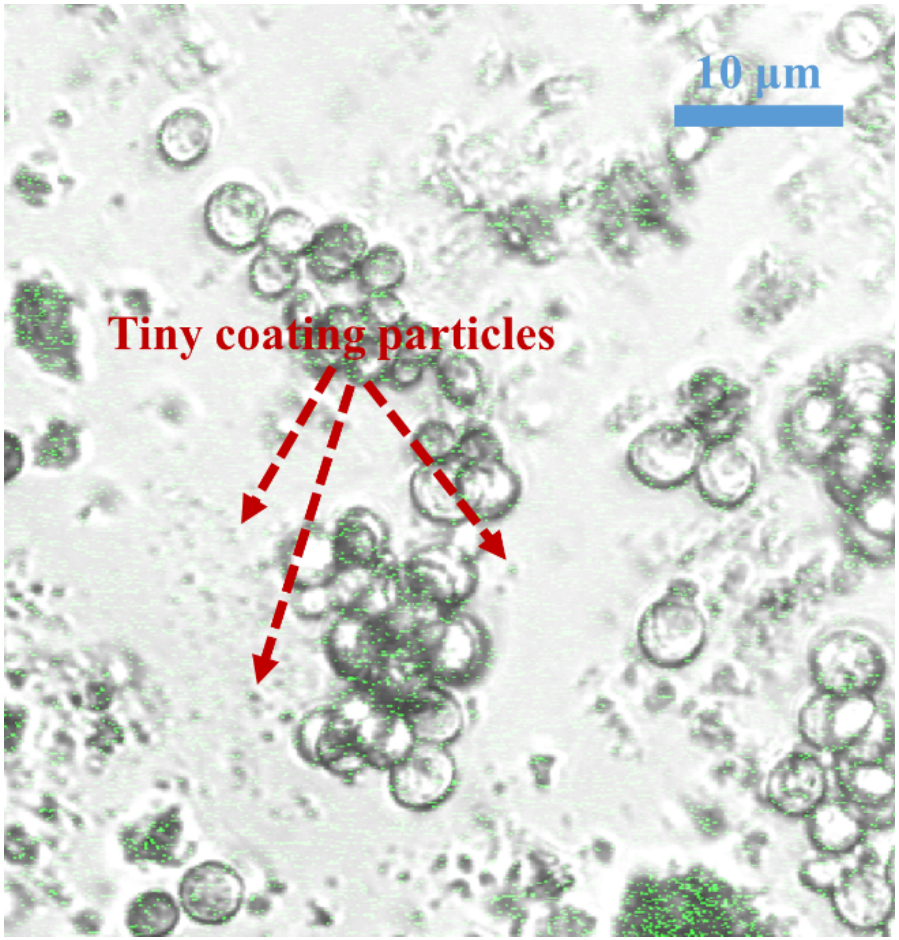

Figure S5. 3D cell cluster growing around along the surface of coated hydrophobic CDs/POSS shell particles.

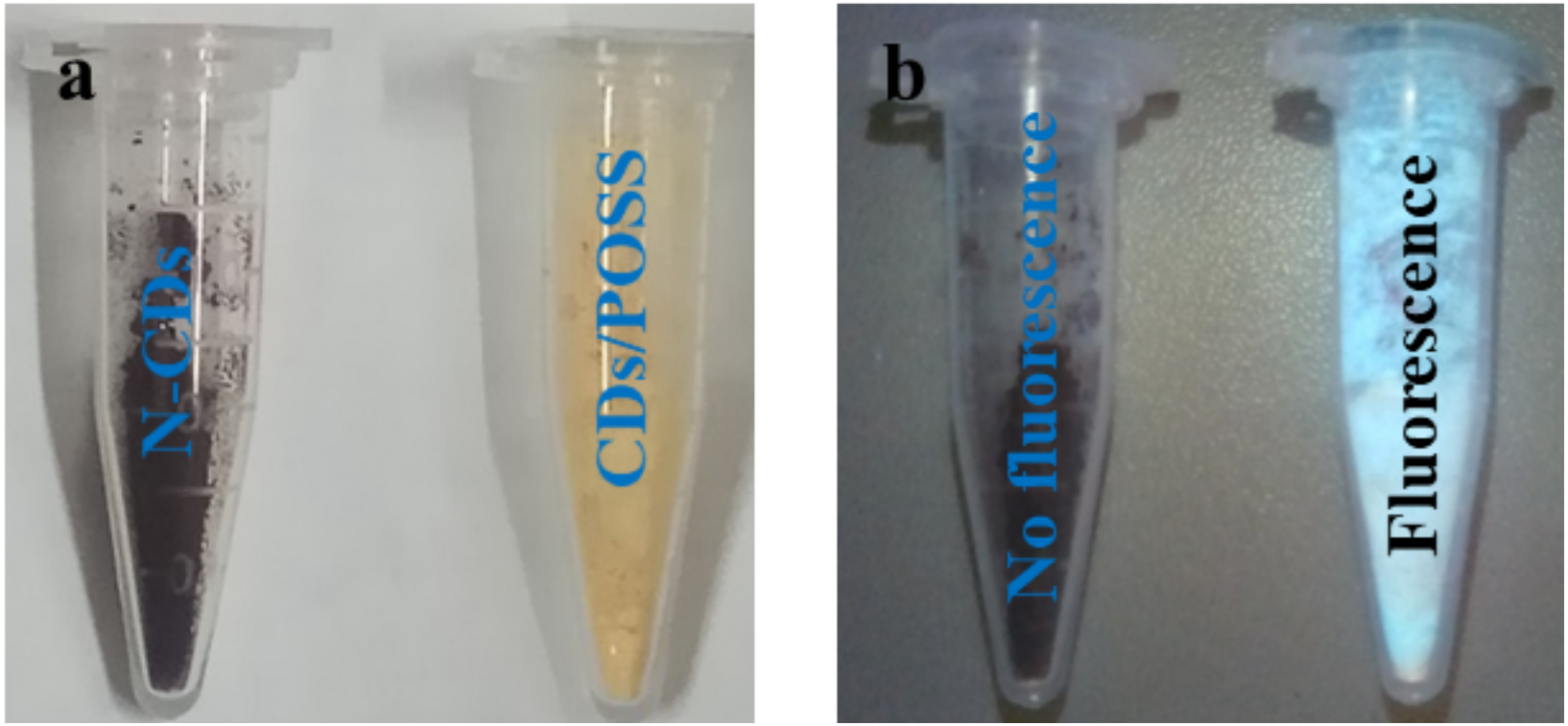

Figure S6. (a) Optical pictures of N-CDs and CDs/POSS, (b) Fluorescence phenomenon of N-CDs and CDs/POSS under excitation of 365 nm